RSC Advances

RSC Publishing

PAPER

View Article Online
View Journal | View Issue

Cite this: *RSC Adv.*, 2013, **3**, 25812

Abiotic reduction of 2-line ferrihydrite: effects on adsorbed arsenate, molybdate, and nickel†

Mario A. Gomez,*[a] M. Jim Hendry,[a] Alauddin Hossain,[a] Soumya Das[a] and Samir Elouatik[b]

Received 29th August 2013
Accepted 15th October 2013

DOI: 10.1039/c3ra44769c

www.rsc.org/advances

The abiotic reduction of X-ferrihydrite (X-FH, where X = 0, As, Mo, or Ni at various Fe/X molar ratios) was investigated by reacting $Fe(II)_{(aq)}$ at solution concentrations of 0.5 mM or 10 mM and at target pH values of 8 or 10 (using lime water as a base) for 7 days. Under all reaction conditions tested, the measured pH was always lower than the target; this difference was greatest for As-FH (at up to 5 pH units). The control FH sample behaved as expected and transformed to lepidocrocite (LP) and goethite (GT) phases. For As-FH, the sample containing less As (Fe/As = 32.9) transformed to LP–GT phases but phase transformation in the sample with more As (Fe/As = 4.47) was inhibited. Solution concentrations of As were below the detection limit for the Fe/As 32.9 sample but As release was evident for the Fe/As 4.47 sample. For Mo-FH, phase transformation to LP–GT phases was observed at lower target pH (8) conditions under both reacting $Fe(II)_{(aq)}$ concentrations. At the higher target pH (10) and using 0.5 mM $Fe(II)_{(aq)}$, phase transformation inhibition was observed for Mo-FH varieties that contained both high (Fe/Mo 12.5) and low (Fe/Mo 31.5) concentrations of Mo. This is the first time an element forming an outer-sphere complex on FH (*e.g.*, Mo) has been shown to retard phase transformation; such phenomena are usually observed for metalloids that form inner-sphere complexes with FH (*e.g.*, As). Under all conditions, Mo was released into solution (up to 340 ppm) and under some conditions was then readsorbed by the solid phase. Finally, all Ni-FH samples exhibited phase transformation under the reaction conditions tested; however, magnetite (MG) and a green rust-like phase were observed in addition to the LP–GT phases. Under all reaction conditions, the largest amount of Ni was released into solution on the first day of reaction, after which the amount in solution decreased with time due to its readsorption into the solid phase.

1. Introduction

Iron is one of the world's most abundant transition metals. Under aqueous oxic conditions, iron generally exists as Fe(III) in the form of hydroxide-oxide phases such as ferrihydrite (FH), lepidocrocite (LP), goethite (GT), hematite (HT), and magnetite (MG).[1] In anoxic aqueous environments, however, the reductive dissolution of these Fe(III) hydroxide-oxide phases generates $Fe(II)_{(aq)}$ ions that can be a dominant control on the oxidation/reduction potential of anaerobic subsurface systems. Such reactions are governed by electron transfer and atom exchange (ETAE) between the $Fe(II)_{(aq)}$ ions and the surface of the Fe(III) hydroxide-oxide solids, which promotes their recrystallization into more crystalline and thermodynamically stable Fe(III)–Fe(III)/Fe(III)–Fe(II) phases (*e.g.*, from ferrihydrite to LP, GT, HT, MG, and/or green rust (GR)).[2–10] With respect to abiotic anoxic reactions of Fe(III) hydroxide-oxide solids, only As-containing Fe(III)-oxide/hydroxide phases (*e.g.*, As-FH, As-GT) and, recently, doped Al–Fe(III)-oxide/hydroxide phases (*e.g.*, FH, GT) have been extensively studied and shown to demonstrate phase transformation inhibition properties with small $As_{(aq)}$ release into solution at particular Fe/As solid molar ratios.[3,9,11–16] These types of properties are of course of interest for the design of stable anoxic toxic element control materials in industrial and natural remediation. However, aside from As-containing-Fe(III)-oxide/hydroxide phases (*e.g.*, FH, GT), the behavior of other metal–metalloids containing varieties on Fe(III)-oxide/hydroxide phases under abiotic anoxic conditions remains largely undocumented. The recent work of Latta *et al.*[17] and Frierdich and Catalano[18] explores the abiotic anoxic reaction behavior of crystalline GT with various ions. Yet to date, no literature has reported similar

[a]*Department of Geological Sciences, University of Saskatchewan, 114 Science Place, Saskatoon, Saskatchewan, S7N 5E2, Canada. E-mail: mag346@mail.usask.ca; Tel: +1-306-2616246*

[b]*Department of Chemistry, University of Montreal, C.P. 6128, Succursale Centre-ville, Montreal, Quebec, H3C 3J7, Canada*

† Electronic supplementary information (ESI) available: Solid elemental composition and analysis of initial materials before reaction, tables summarizing element release and percentages of X element remaining in solution, individual test data and phase transformation summary observed for all the reaction conditions. pH profiles for all the X-FH varieties reacted under all the reaction conditions, TEM and Raman data for selective samples discussed in the text are also presented. See DOI: 10.1039/c3ra44769c

work on FH with other elements that may be encountered aside from As (*e.g.* Mo and Ni).[17–19] Implications of the reductive dissolution of bulk crystalline and nano-crystalline Fe(III) hydroxide-oxide phases (*e.g.*, GT and FH) arise with respect to the release (into the aqueous phase) of trace elements and contaminants involved structurally or as adsorbed cations and/or molecules (*e.g.*, Ni(II), Cu(II), Co(II), Mn(II), PO_4, AsO_4, CO_3, SiO_3, and organic matter).[11,13,17–21]

An understanding of the effects of reductive dissolution of ferrihydrite with adsorbed and/or structurally-incorporated trace elements (elements of concern, EOCs) is important with respect to their long-term sequestration in mining and mill tailing operations. For example, the milling of uranium (U) ore has to date resulted in the generation of about one billion tons of tailings at 4000 mines worldwide.[22] The world's largest and richest reserves of U ore are found in the Athabasca Basin of northern Saskatchewan, Canada. Tailings from these mining operations have been deposited subaqueously in engineered in-pit tailings management facilities (TMF) constructed from mined out ore bodies (in-pit) since 1983. These tailings are oxic ($E_h \sim +200$ mV),[23,24] even after more than 30 years in the TMFs. These tailings typically contain large masses of EOCs, including As, Mo, and Ni, which are sequestered in the tailings solids *via* adsorption or co-precipitation with secondary 2-line ferrihydrite.[23–31] Because U tailings can contain elevated concentrations of long-lived (up to tens of thousands of years) transuranic elements (*i.e.*, Pu isotopes and Am),[24] a 10 000 year design criteria for TMFs handing U tailings has been established.[32] This containment criterion also applies to the geochemical stability of EOCs in the TMFs, including potential impacts due to reductive dissolution of ferrihydrite.

The objective of the present study was to evaluate the stability of As, Mo, and Ni adsorbed onto ferrihydrite under anoxic environments (in presence of $Fe(II)_{(aq)}$), over a range of pH conditions and at concentrations typically observed in U tailings. It should be noted that the term "stability" in our case refers to the phase transformation of FH to other crystalline Fe(III)–Fe(III)/Fe(II)–Fe(II) phases (*e.g.* LP, GT, HT, MG) in the presence of $Fe(II)_{(aq)}$, and the release of EOCs (As, Mo and Ni) into solution as a consequence of this phase transformation. Such objectives were attained *via* batch experiments and subsequent analysis of both the aqueous and solid phases. Results from the simple synthetic experiments presented here provide information on how the long-term stability of As/Mo/Ni adsorbed ferrihydrite systems (typically found in U mills and TMFs of northern Canada) may behave if subjected to anoxic reducing conditions. The results are applicable to tailings deposits in general and provide baseline data upon which abiotic experiments of more mineralogically complex U tailings will be developed.

2. Experimental

2.1 Synthesis of 2-line ferrihydrite and adsorption of As, Mo, and Ni

Samples of FH were prepared at room temperature (21 °C) using the method of Cornell and Schwertmann[1] but with reagent grade ferric sulfate salt ($Fe_2(SO_4)_3 \cdot xH_2O$ Sigma-Aldrich) used to precipitate FH to simulate the dominant anion (SO_4) present in northern Canadian U tailings.[23] Briefly, $Fe_2(SO_4)_3 \cdot xH_2O$ was dissolved in deionized water to create a 0.3 M solution of $Fe(III)_{(aq)}$. The pH of the solution was then increased to 7.5 over 5 min using 1 M NaOH; thereafter, the pH was maintained at 7.5 for 1 h while the slurry was vigorously agitated. The supernatant was then removed *via* pressure filtration (Hazardous Waste Pressure Filter System, Millipore) using N_2 and a 0.2 μm membrane filter (EMD Millipore Corp.). To remove SO_4 during the FH synthesis, the wet filtered solids were placed in 1000 mL deionized water and stirred overnight (12 h), after which the supernatant was removed using the pressure filter system described above. This procedure was then repeated. After the second wash, the wet solids were placed in solutions containing analytical-reagent grade $As_2O_5 \cdot xH_2O$, $NiSO_4 \cdot 6H_2O$, or $Na_2MoO_4 \cdot 2H_2O$ (Sigma-Aldrich) at concentrations sufficient to achieve high (4–10) and low (30–60) adsorbed Fe/X molar ratios; a control sample had a Fe/X molar ratio of 0 (no EOCs added) (Table S0†). The solutions of the analytical-reagent grade $As_2O_5 \cdot xH_2O$, $NiSO_4 \cdot 6H_2O$, or $Na_2MoO_4 \cdot 2H_2O$ (Sigma-Aldrich) at the desired concentrations were prepared by dissolving the hydrated salt in deionized water (18 mΩ) and stirring overnight to ensure it dissolved completely before its addition to the wet ferrihydrite solids. These molar ratios were selected to approximate the range reported for mill raffinates and tailings[26,27,33] and resulted in products labeled hereafter as follows: Fe/As 4.47, Fe/As 32.9, Fe/Mo 12.4, Fe/Mo 31.5, Fe/Ni 14.9, and Fe/Ni 61.5. After stirring overnight, the slurries (pH 3.5) were pressure filtered as described above. The wet solids were then air dried for 24 h at ambient temperature, after which they were characterized using inductively coupled plasma mass spectrometry (ICP-MS), X-ray diffraction (XRD), and Raman spectroscopy to confirm the FH phase as well as the mass of adsorbed contaminants (Fig. S1; Table S0†). Dried samples were also transferred to a glove box (UNIlab station from MBraun, Germany; 100% N_2) for abiotic reduction tests.

LP, GT, GR, and MG were also synthesized according to published methods[1,35] for comparison with the abiotic reaction products.

2.2 Abiotic batch reactions

Abiotic Fe(II) redox reactions of FH and EOC-adsorbed FH were conducted in duplicate and in some cases triplicate (for phase confirmation) using $Fe(II)SO_4 \cdot 7H_2O$ (Fisher Scientific) as the Fe(II) catalyst. $Fe(II)_{(aq)}$ was made by dissolving the Fe(II) $SO_4 \cdot 7H_2O$ salt in deoxygenated deionized water (pH ~ 6) to yield a 10 mM stock solution. Prior to using this stock solution to make the 0.5 mM solution, it was inspected after sitting overnight to confirm no yellow colour (indicative of Fe(II) oxidation).[11] A final confirmation that $Fe(II)_{(aq)}$ was active in solution was done using Fe^{2+} Quant Test Strips (Sigma-Aldrich). The presence of red and the degree of color saturation in the strip was indicative of the Fe^{2+}–cyano complex that forms and the approximate concentration range, respectively; red colour was confirmed for both 0.5 and 10 mM solutions and the degree of saturation was greater in the latter case. $Fe(II)_{(aq)}$ concentrations were inferred from measurements of the total Fe in solution *via* ICP-MS. Note that we

can equate the amount of $Fe(II)_{(aq)}$ and the measured total Fe in our reacting solutions because all were prepared in the glove box where no Fe(III) was present and we used pure ferrous sulfate hydrated salt as an $Fe(II)_{(aq)}$ source. This is not the case for the final solution from the reaction in which both $Fe(III)_{(aq)}$ and $Fe(II)_{(aq)}$ exist due to the dissolution of the X-FH; as such, we cannot in these cases equate the $Fe(II)_{(aq)}$ content with the total Fe content. Preliminary tests conducted using only the aqueous Fe(II) solutions (no Fe/X solids) demonstrated the formation of undesirable precipitates (likely $Fe(OH)_{2(s)}$) at concentrations >10 mM $Fe(II)_{(aq)}$ at pH 8 and >0.5 mM $Fe(II)_{(aq)}$ at pH 10 (Fig. S2†). As such, further experiments were only conducted at $Fe(II)_{(aq)}$ concentrations of 0.5 and 10 mM at pH 8 and 0.5 mM at pH 10; these pH values represented typical conditions in the U mill and the discharged tailings, respectively. Corresponding concentrations of Fe/X solids were added to make up $Fe(II)_{(aq)}/Fe(III)_{(s)}$ reacting ratios of 1.6 and 33.

The EOC-adsorbed FH solids, $Fe(II)SO_4 \cdot 7H_2O$, and $Ca(OH)_2$ (Sigma-Aldrich) as well as deoxygenated–deionized water (produced by bubbling with $N_{2(g)}$ for 2 h) were placed in the glove box for 3 days to scrub adsorbed or dissolved oxygen from the solids and solutions prior to use. After this 3-day period, saturated lime water was created in the glove box by dissolving 10 g of reagent grade $Ca(OH)_2$ (Sigma-Aldrich) in 1000 mL of the deoxygenated deionized water. To create the test solutions, 40 mL of the $Fe(II)_{(aq)}$ solution were transferred into 150 mL glass beakers, the pH adjusted with the lime water to the target pH (8 or 10 $\pm$ 0.1), and 400 mg of the desired EOC-adsorbed FH solid added. The pH was again measured and adjusted each day to attain the target pH of 8 or 10. The reactions were allowed to proceed for 7 days to ensure completion of the reduction reactions and to emulate a TCLP-like leachability test[36] of the EOCs. Similar reactions have been documented to occur in hours[3,11] and, as such, a 7-day period was considered sufficient for our purposes. The pH was measured and readjusted to the target pH every day during the reaction period (see ESI† for pH measured profiles). All pH ranges reported are the mean of duplicate tests.

One mL of aqueous sample was collected and measured *via* ICP-MS from each reaction vessel using a 10 cm^3 syringe with a 0.02 μm filter (Whatman Inc.) on day 1, 2, 4, and 7 of the experiment. For all solution data, we only report the total element concentration and do not partition into the possible redox states that may occur in solution (*e.g.*, Fe(II) and Fe(III)). Concentrations or percentages reported for elements of interest in solution represent the mean of duplicate tests. After aqueous sample collection on day 7, the remaining solution was separated from the solid *via* decantation and the solid left inside the glove box to dry at ambient temperature. Solid samples were then powdered using a mortar and pestle in the glove box and subsamples collected and stored for analysis using the elemental, molecular, and structural techniques described below. All experiments were conducted at ambient temperature.

2.3 Analytical methods

X-ray diffraction and micro-Raman spectroscopic analyses were conducted on the initial and final (day 7) reacted solids (FH and the EOC-adsorbed FHs). For XRD measurements, a small amount of methanol (600 μL) was added to ground dried powder subsamples to create a thin paste. This paste was then dropped onto a flat glass sample holder, evenly distributed, and allowed to dry for 5 min. Measurements were conducted using a PANalytical Empyrean instrument with a rotating anode (2.7 kW) and a Co target (λ Cu $K_\alpha = 1.7902$ Å) using a graphite monochromator, operating at 40 kV and 45 mA. Scanning took place between 10 and 80 deg 2θ with a 0.01 deg step and scan step time of 85 s. Phase detection limits for lab-based XRD generally range from 1–5 wt%.[37]

Phase identification was conducted using the Phase-ID function in X'pert HighScore Plus software and the corresponding Joint Committee on Power Diffraction Standards (JCPDS) database reference data for FH (PDF 98-007-6750 and 98-011-1017), LP (PDF 98-001-2041), GT (PDF 98-003-4786), MG (98-011-7729), fougerite (PDF 98-011-2393), and HT (PDF 98-011-9589). In addition, XRD analyses were conducted on commercial reagent grade GT (CAS no. 1310-14-1), LP (CAS no. 12022-37-6), and MG (CAS no. 1309-38-2).

Micro-Raman spectroscopic analysis was conducted using a Renishaw InVia Raman microscope equipped with a polarized argon laser operating at 514 nm. The laser delivered 25 mW at the laser exit and 8 mW at the sample using the 50× short distance objective (gives a pot size of ~1 μm). Five scans were collected from 150 to 1400 cm^{-1} and the average taken to improve the resolution and the statistics of the collected data. The energy resolution was 4 cm^{-1} at the full width half max of the internal Si reference peak. The scans were collected at 10% of the laser output at the microscope exit to minimize radiation damage or local induced heat transformation of FH to HT or MG.[38] The system was calibrated to the 520 cm^{-1} Si peak (for position and intensity) before data collection. Phase detection limits for micro-Raman are typically on the order of 1 wt%.[39] Data collection and spectral treatment were performed with WiRE 2.0 software from Renishaw. For all samples, three to five random areas were probed to ensure that the phase(s) were consistent throughout the sample. The Raman data presented include two spectra from the various spots probed in the reacted samples to show the mixture of phases.

Transmission electron microscopy (TEM) images were collected on a select set of powdered solids from the end of the experiment (day 7) using a Philips CM-200 microscope operating at 200 kV. The samples were prepared by dropping dilute solutions of the subsample in ethanol onto 400-mesh carbon-coated copper grids and evaporating the solvent to dryness before sample analysis. TEM was only used to verify if crystallization after reaction[3] and not to characterize the phase(s) produced.

Bulk elemental analysis of all aqueous and solid samples was conducted using a Perkin-Elmer Elan 5000 ICP-MS instrument with a relative standard deviation (RSD) of ±10%. Solid samples were digested in an acidic media ($HF–HNO_3$), left overnight to dissolve, and diluted accordingly for analysis of Fe, Al, Mg, Ni, Se, As, and Mo.[40,41] All concentrations or percentages reported represent the mean of duplicate tests. The percentage of an X element (X = 0, As, Mo and Ni) remaining in the solid was

calculated from the average highest concentration of element X released in the solution for the 7-day period and the initial amount of X element in the solid (Tables S0–S3†). A similar calculation was done for the percentage of $Fe(II)_{(aq)}$ remaining in solution after the 7-day reaction period (Tables S1–S3†). Individual leachability data from all reaction conditions investigated are presented in the ESI (Tables S4–S6†).

3. Results and discussion

3.1 Reactions at a target pH of 8 using 10 mM $Fe(II)_{(aq)}$

In the reaction vessel containing only pure FH, the pH deviated from the target pH of 8 and resulted in a pH range of 6.5–7.1 throughout the experiment. The total Fe concentration in solution (as $Fe(II)_{(aq)}$) decreased slowly (in relation to other cases discussed below) until the end of the reaction period, by which time an average of 81% had been removed (Table 1).

Powder XRD data and phase analysis *via* X'pert Highscore of the solid phase at day 7 (Fig. 1) indicated a considerable mass of unreacted FH as well as the presence of GT and lesser amounts of LP. Micro-Raman analysis confirmed the presence of GT and LP and also demonstrated that the phase transformation did not occur uniformly on the particle surfaces; FH, GT, LP, and mixtures thereof were all observed, possibly due to the varying conversion kinetics of different particles as related to their distinct surface characteristics. The inhomogeneous phase formation on the particle surfaces was also evident under light microscope, where various colors from light brown-LP to dark brown-GT and/or FH were observed (Fig. S3†). These findings are consistent with literature predictions for the measured average pH range of the samples.[3,11,14–16,42] MG was expected to be a dominant phase at the target pH of 8,[3] but only GT and LP were observed because the measured average pH range was <8 throughout the 7-day reaction period.

For the As-FH samples, the pH variability and the decrease from the target pH of 8 was pronounced for both Fe/As 4.47 and Fe/As 32.9. The greatest pH decrease was observed for Fe/As 4.47 (average pH range of 5.4 to 7.2). This lowering of solution pH usually results from the dissolution of arsenic (*e.g.*, from Fe(III)-arsenates[43]), which causes the formation of protonated aqueous arsenic complexes. No correlation between time and As release was observed for the Fe/As 4.47 and Fe/As 32.9 samples. For the Fe/As 4.47 sample, a small release of arsenic (average 0.53 ppm As) into solution (Tables 1 and S0†) was observed but 99% of the original As remained in the solid at the end of the 7-day reaction period (Table S0†). The large amount of arsenate remaining in the solid after the reaction was also evident from the arsenate band at 843 cm^{-1} in the Raman spectrum (Fig. 1). No measurable As release was observed for the Fe/As 32.9 sample, which is contrary to prior reports for similar solid Fe/As molar ratios.[11–13] This lack of As release for the Fe/As 32.9 sample may be due to a smaller amount of covalently bound As on FH available for release into solution (*versus* the Fe/As 4.47) or the readsorption of any released into the solid phase (composed of new GT/LP phases and unreacted FH). By the end of the 7-day reaction period, 98 and 88% of the total Fe added (as $Fe(II)_{(aq)}$) was removed from solution for the Fe/As 4.47 and Fe/As 32.9

Table 1 Leachability of Fe and elements of concern (X = As, Mo, and Ni) for tests conducted at pH 8 for 7 days with 10 mM $Fe(II)_{(aq)}$. Time 0 days represents conditions before Fe/X solids were added. Concentration units for (Fe) and (X) are in ppm. The values reported are the average of the two duplicate tests along with their standard deviations. Individual test data may be found in the ESI

Time	Ferrihydrite		Fe/As 4.47			Fe/As 32.9			Fe/Mo 12.4			Fe/Mo 31.2			Fe/Ni 14.9			Fe/Ni 61.5		
(days)	pH	(Fe)	(X)	pH	(Fe)	(X)	pH	(Fe)	(X)	pH	(Fe)	(X)	pH	(Fe)	(X)	pH	(Fe)	(X)	pH	(Fe)	(X)
0	5.5 ± 0.1	749 ± 0	0	5.5 ± 0.1	749 ± 0	0	5.5 ± 0.1	749 ± 0	0	5.5 ± 0.1	749 ± 0	0	5.5 ± 0.1	749 ± 0	0	5.5 ± 0.1	749 ± 0	0	5.5 ± 0.1	749 ± 0	0
1	6.5 ± 0.1	424 ± 21.9	0	5.4 ± 0.2	284 ± 9.2	0.4 ± 0.2	7.1 ± 0.5	385 ± 80.6	0	7.5 ± 0.3	196 ± 30.4	25.5 ± 3.3	7.2 ± 0.1	368 ± 32.5	0 ± 0	6.7 ± 0.1	347 ± 0.1	7.6 ± 0.8	7.3 ± 0.3	31.8 ± 0.1	1.18 ± 0.1
2	6.5 ± 0.1	412 ± 12.0	0	6.8 ± 0.2	144 ± 16.2	0.2 ± 0	7.0 ± 0.2	286 ± 38.1	0	7.3 ± 0.3	145 ± 34.6	15.7 ± 4.0	7.4 ± 0	339 ± 36.7	0 ± 0	7.1 ± 0.1	28.8 ± 7.0	4.0 ± 0.2	7.5 ± 0.1	22.2 ± 9.9	0.99 ± 0.1
4	7.1 ± 0.1	319 ± 4.9	0	6.3 ± 0.7	30.9 ± 4.4	0.3 ± 0.2	7.3 ± 0.4	207 ± 53.0	0	7.6 ± 0.1	97 ± 39.5	9.0 ± 4.0	7.3 ± 0.4	171 ± 1.4	0 ± 0	7.1 ± 0	13.5 ± 2.9	2.1 ± 0.9	7.2 ± 0.2	12.3 ± 1.7	0.92 ± 0
7	6.5 ± 0.1	140 ± 57.2	0	7.2 ± 0.6	11.4 ± 1.3	0.4 ± 0.2	7.2 ± 0.1	87.7 ± 12.3	0	7.4 ± 0.3	67.5 ± 54.3	1.8 ± 0.9	7.1 ± 0.6	160 ± 1.3	0 ± 0	7.2 ± 0.1	8.0 ± 0	1.0 ± 0.1	7.5 ± 0.1	4.35 ± 2.2	0.34 ± 0.1

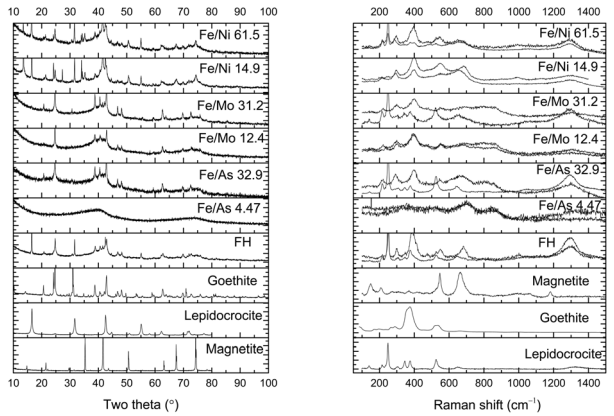

Fig. 1 Powder X-ray diffraction spectra (left) and micro-Raman spectra (right) of solid products reacted at a target pH of 8 for 7 days with 10 mM $Fe(II)_{(aq)}$. Spectra of relevant standard materials are shown for comparison. For each reacted sample, two Raman spectra are presented to show the mixtures of phases found in the reacted sample.

samples, respectively (Table 1). The Fe/As 4.47 sample showed no phase transformation (Table S7,† Fig. 1) at the macro-scale (*via* XRD and micro-Raman) or nano-scale (*via* TEM; Table S7 and Fig. S5†) in agreement with existing literature.[12] Such inhibition of phase transformation has been reasoned to result from the large amount of As covalently bonded to the surface of FH, which can block electron transfer reaction sites on FH.[44] Similar reasoning has been used to explain the inhibition of phase transformation in co-precipitated systems.[11] In the case of the Fe/As 32.9 sample, only LP and GT phases were observed to form, in contrast to Erbs *et al.*[12] who only report the presence of 6-line FH. The LP and GT phases observed in our case align with our measured average pH (range 6.9–7; Fig. S4†) and the formation pH of LP and GT.[3] The differences between our work and Erbs *et al.*[12] may stem from their lower reaction pH and use of hydroquinone as an electron donor instead of $Fe(II)_{(aq)}$.

No reports have been published with respect to the abiotic reductive dissolution of adsorbed Mo-FH types. In our batch experiments, the pH decrease from the target pH of 8 was less pronounced for Mo-FH than for As-FH. The Fe/Mo 12.4 and Fe/Mo 31.5 samples had measured average pH values ranging from 7.3 to 7.6 and 7.1 to 7.4, respectively. The amount of Mo released into solution was higher for the Fe/Mo 12.4 sample *versus* the Fe/Mo 31.5 sample (Table 1). For both cases, the majority of the Mo was released into solution on the first day of reaction, after which the amount released decreased. This decrease in Mo concentrations with time may be attributed to its readsorption onto new crystalline LP and/or GT phases and/or unreacted FH (Table 1, Fig. 1). The average fraction of Mo remaining in the solid by the end of the reaction period was 99% for both the Fe/Mo 12.4 and Fe/Mo 31.5 samples. An average of 91 and 78% of the total Fe (as $Fe(II)_{(aq)}$) was removed from solution by the end of the reaction period for Fe/Mo 12.4 and Fe/Mo 31.5, respectively (Table 1). Phase transformation to LP and/or GT was observed for both the Fe/Mo 12.4 and Fe/Mo 31.5 samples and a noticeable amount of unreacted FH remained in both cases (Table 1, Fig. 1 and S5†). No MG was observed for either sample because the average pH during the 7-day reaction period was always <8. The fact that phase transformation occurred for both Fe/Mo 12.4 and Fe/Mo 31.5 samples indicates that, under these conditions, Mo (as MoO_4) adsorbed onto FH cannot sufficiently block electron transfer reaction sites from the electron donor ($Fe(II)_{(aq)}$) to prevent phase transformation, as compared to the As-FH system.[11–13] This latter observation may be explained in part by the type of bonding that occurs in As-FH *versus* Mo-FH: As adsorbs onto FH covalently *via* bidentate bridging[45] while Mo adsorbs onto FH *via* non-covalent outer-sphere bonding.[46,47] Therefore, the displacement of covalently bonded As on FH by the $Fe(II)_{(aq)}$ ions in solution is expected to be more difficult than for Mo on FH, for which only electrostatic forces (outer-sphere bonding) exist.

For the Fe/Ni 14.9 and Fe/Ni 61.5 samples, average pH ranges of 6.7 to 7.2 and 7.2 to 7.5 were measured over the course of the experiment. This decrease from the target pH of 8 was less than observed for the As-FH cases (Fig. S4†). The measured Ni release into solution was greater for the Fe/Ni 14.9 sample relative to the Fe/Ni 61.5 (Table 1), and 99% of the Ni remained in the reacted solid by the end of the 7-day reaction period. For both samples, the amount of Ni released into solution was greatest on the first day of reaction, after which it slowly decreased (Table 1). For Ni-FH systems, EXAFS data[48] show that the Ni atoms bond to the O–Fe of ferrihydrite *via* edge-sharing surface (Fe–O–Ni 3.0 Å) and edge-sharing (Fe–O–Ni 3.2 Å) bonded species with a small amount of corner sharing species (Fe–O–Ni 4.0 Å). Therefore, the release of Ni in our case may be attributed to the displacement of weakly bonded corner sharing Ni species, which are displaced by the $Fe(II)_{(aq)}$ ions. This Ni decrease with time in solution is similar to Mo (described above) and can also be attributed to readsorption onto newly formed LP and/or GT and/or unreacted FH (Fig. 1). The total Fe (as $Fe(II)_{(aq)}$) removed from solution was 98% and 99% for the Fe/Ni 14.9 and Fe/Ni 61.5 samples, respectively. XRD and micro-Raman analysis confirm phase transformations occurred for both Fe/Ni 14.9 and Fe/Ni 61.5 samples by the end of the reaction period (Table S7,† Fig. 1). In the case of Fe/Ni 61.5, LP was favored; in the case of Fe/Ni 14.9, GT dominated. Interestingly, MG was observed (*via* XRD and Raman) for both the Fe/Ni 14.9 and 30 samples despite the pH being <8 (Fig. S4†). This observation indicates that the presence of Ni on FH favors the formation of MG at pH values <8.[3]

3.2 Reactions at a target pH of 8 using 0.5 mM $Fe(II)_{(aq)}$

Because fewer $Fe(II)_{(aq)}$ ions are in solution at concentrations of 0.5 mM (Table 2), the total Fe (as $Fe(II)_{(aq)}$) uptake by the solid FH at the end the reaction period was 99% and the measured average reaction pH ranged from 6.7 to 7.1. Phase analysis of the reacted FH *via* XRD and micro-Raman spectroscopy (Fig. 2) showed the presence of LP and/or GT (Table S8†).

MG formation was not observed, again due to lower pH values that favor the formation of LP and GT (Fig. S6†). Inhomogeneous phase formation was observed on the surfaces of

Table 2 Leachability of Fe and elements of concern (X = As, Mo, and Ni) for tests conducted at pH 8 for 7 days with 0.5 mM $Fe(II)_{(aq)}$. Time 0 days represents conditions before Fe/X solids were added. Concentration units for (Fe) and (X) are in ppm. The values reported are the average of the two duplicate tests along with their standard deviations. Individual test data may be found in the ESI

Time	Ferrihydrite			Fe/As 4.47			Fe/As 32.9			Fe/Mo 12.4			Fe/Mo 31.2			Fe/Ni 14.9			Fe/Ni 61.5		
(days)	pH	(Fe)	(X)	pH	(Fe)	(X)	pH	(Fe)	(X)	pH	(Fe)	(X)	pH	(Fe)	(X)	pH	(Fe)	(X)	pH	(Fe)	(X)
0	5.5 ± 0	38 ± 0	0	5.5 ± 0	38 ± 0	1 0	5.5 ± 0	38 ± 0	1 0	5.5 ± 0.1	38 ± 0	0	5.5 ± 0.1	38 ± 0	0	5.5 ± 0	38 ± 0	0	5.5 ± 0	38 ± 0	0
1	6.7 ± 0.6	6.8 ± 0.9	0	5.6 ± 0.1	7.1 ± 3.2	13.3 ± 3.5	6.9 ± 0.6	9.41 ± 0.1	0	7.9 ± 0	0.03 ± 0	247 ± 38.9	7.8 ± 0	3.9 ± 5.3	3.4 ± 0.2	7.2 ± 0	17.5 ± 4.7	158 ± 31.8	7.3 ± 0	24.3 ± 10.6	23.3 ± 6.4
2	7.1 ± 0.6	4.1 ± 0.7	0	5.7 ± 0.3	2.2 ± 0.9	17.8 ± 0	7.2 ± 0.1	7.68 ± 0.1	0	8.2 ± 0.1	0.02 ± 0	260 ± 0	7.8 ± 0	0 ± 0	8.1 ± 6.4	7.7 ± 0.1	1.7 ± 0	58.0 ± 7.3	7.4 ± 0.1	13.5 ± 7.9	12.8 ± 2.2
4	6.9 ± 0.4	1.0 ± 0.1	0	6.1 ± 0.1	0.5 ± 0.9	30.8 ± 2.0	7.2 ± 0.3	5.04 ± 0.1	0	8.0 ± 0.1	0.02 ± 0	308 ± 0.7	8.0 ± 0.2	0 ± 0	10.4 ± 7.7	7.8 ± 0.1	1.4 ± 0	40.7 ± 2.5	7.6 ± 0	9.65 ± 5.6	14.8 ± 1.0
7	6.7 ± 0.2	0.3 ± 0	0	6.1 ± 0.1	0.2 ± 0.1	31.2 ± 1.9	6.7 ± 0.3	1.42 ± 0.1	0	8.0 ± 0.1	0.02 ± 0	340 ± 0.7	7.7 ± 0.1	0 ± 0	11.2 ± 6.9	7.9 ± 0.2	0.7 ± 0	12.6 ± 2.7	7.6 ± 0.1	4.64 ± 1.8	10.6 ± 2.7

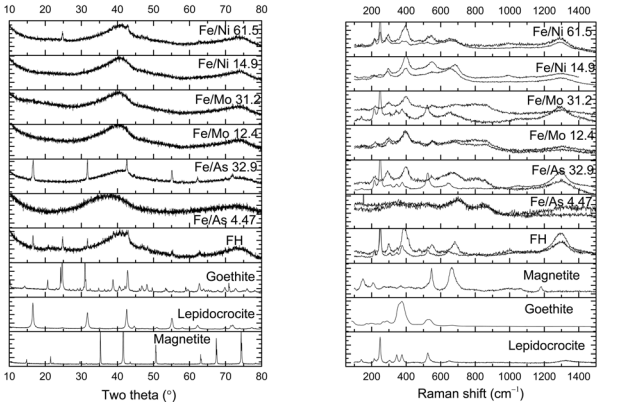

Fig. 2 Powder X-ray diffraction spectra (left) and micro-Raman spectra (right) of solid products reacted at a target pH of 8 for 7 days with 0.5 mM $Fe(II)_{(aq)}$. Spectra of relevant standard materials are shown for comparison. For each reacted sample, two Raman spectra are presented to show the mixtures of phases found in the reacted sample.

the FH particles (Fig. S3†) but was much less pronounced than for experiments conducted with 10 mM $Fe(II)_{(aq)}$.

For the As-FH samples, the measured pH decrease from the target pH of 8 was significant. The pH of the Fe/As 4.47 sample was as low as 5.6 to 6.1 while for the Fe/As 32.9 sample was 6.7 to 7.2. No measurable As was released into solution for the Fe/As 32.9 sample, while an average of 31.2 ppm As was released from the reacted Fe/As 4.47 sample (Table 2). In both cases, an average of 99% of the As remained in the solid by the end of the 7-day reaction period. This arsenate presence after the reaction can be further confirmed from the arsenate band at 850 cm^{-1} in the Raman spectrum (Fig. 1). Notably, the As released into solution for the Fe/As 4.47 sample reacted with 0.5 mM $Fe(II)_{(aq)}$ was higher than for the same solid reacted with 10 mM $Fe(II)_{(aq)}$. This may arise due to a larger number of $Fe(II)_{(aq)}$ ions being adsorbed by the FH surface (99% of the total Fe (as 0.5 mM $Fe(II)_{(aq)}$) was removed from solution) *via* displacement of As at lower $Fe(II)_{(aq)}$ concentrations (*e.g.*, 0.5 mM). In contrast, higher concentrations of $Fe(II)_{(aq)}$ (*e.g.*, 10 mM) could result in a solution richer in $Fe(II)_{(aq)}$ ions, which may combine with the released $As_{(aq)}$ ions to form Fe(II)–As aqueous complexes[33,34] that are adsorbed on the FH surface and, as a result, become immobilized. The As released into solution for the Fe/As 4.47 case increased with time and these $As_{(aq)}$ ions did not readsorb onto the unreacted solid FH phase after 7 days of reaction. This lack of As readsorption may be due to the unavailability of new LP and/or GT surfaces in the Fe/As 4.47 system as a result of the phase transformation inhibition observed. The total Fe (as $Fe(II)_{(aq)}$) removed from solution by the end of the reaction period was 83% and 96% for the Fe/As 4.47 and Fe/As 32.9 samples, respectively. Again, the Fe/As 4.47 sample showed phase transformation inhibition at the macro-scale (XRD, micro-Raman) and nano-scale (TEM) (Fig. 2 and S7†), while the Fe/As 32.9 sample showed only the presence of LP.

For the Mo-FH cases, average pH ranges of 7.9–8.2 and 7.7–8.0 were observed for the Fe/Mo 12.4 and Fe/Mo 31.5 samples,

respectively. In both cases, an average of 99% of the Mo remained in the final reacted solid and the same amount (99%) of total Fe (as $Fe(II)_{(aq)}$) was removed from solution by the end of the 7-day reaction period (Table 2). However, average concentrations of 340 and 11 ppm of Mo were released into solution from the Fe/Mo 12.4 and Fe/Mo 31.5 samples, respectively (Table 2). The significant amounts of Mo released into solution from the Fe/Mo 12.4 sample are of concern because they exceed the acceptable health limits in water systems.[49] At the target pH of 8, more Mo was released into solution with $Fe(II)_{(aq)}$ concentrations of 0.5 mM than the previously discussed 10 mM $Fe(II)_{(aq)}$ (Tables 1 and 2). Such findings suggest that lower concentrations of $Fe(II)_{(aq)}$ are more effective at displacing the weak outer-sphere complex between Mo and FH. Furthermore, both the Fe/Mo 12.4 and Fe/Mo 31.5 samples reacted with 0.5 mM $Fe(II)_{(aq)}$ at a target pH of 8 had concentrations of Mo released into solution that increased with time (*i.e.*, no readsorption onto the solid phase was observed at the end of the 7-day reaction period (Table 2). This lack of readsorption for Fe/Mo 31.5 is interesting because new available LP and/or GT surfaces are formed as a result of the phase transformation and may have been used as attachment sites for the released aqueous Mo (Fig. S6†). Therefore, the observed lack of readsorption may arise from $Fe(II)_{(aq)}$ ions occupying most of the reaction sites where the Mo resided on the FH surface regardless of whether or not new surfaces arose from LP and/or GT formation (more data are needed to confirm this in future work). Notably, phase analysis *via* XRD and micro-Raman for Fe/Mo 12.4 and Fe/Mo 31.5 samples showed no phase transformation to the expected LP and/or GT phases (Fig. 2, Table S8†). This lack of phase detection may result from instrument-method insensitivity. Such phase transformation processes can occur at low concentrations (*e.g.*, <1 wt%) and scales (nano). Further investigations were therefore conducted at the nano-scale *via* TEM analysis, the data from which demonstrate the clear formation of nano-scale LP and/or GT crystalline sharp phases created from the FH matrix (Fig. S7†). These data suggest that the lack of Mo readsorption observed under these conditions may indeed result from the direct surface substitution of Mo sites on FH by the $Fe(II)_{(aq)}$ ions, which then initiate the catalytic formation of nano-scale LP and/or GT phases.

For the Ni-FH samples, the decrease in pH from the target of 8 was minimal, with measured average pH values ranging from 7.2 to 7.9 for Fe/Ni 14.9 and 7.3 to 7.9 for Fe/Ni 61.5. The average total amount of Fe (as $Fe(II)_{(aq)}$) removed from solution was 98 and 87% for the Fe/Ni 14.9 and Fe/Ni 61.5 samples, respectively. In both cases, an average of 99% of the Ni remained in the solid phase by the end of the 7-day reaction period while an average of 58.5 and 23.2 ppm of Ni was released into solution from the Fe/Ni 14.9 and Fe/Ni 61.5 samples, respectively. The maximum concentration of Ni was released in solution after the first day of reaction, after which time it decreased (Table 2). This release of Ni may be attributed to the displacement of weakly bonded Ni species on the surface of FH by the $Fe(II)_{(aq)}$ ions. The readsorption behavior is attributed to the reattachment of the Ni released from solution to the newly formed phases (*e.g.*, LP and/or GT and/or GR)[50,51] and unreacted FH. This Ni release and readsorption behavior was also observed at higher concentrations of 10 mM $Fe(II)_{(aq)}$ and a target pH of 8 (Table 1). Phase analysis *via* XRD failed to show any phase transformation, but micro-Raman spectroscopy indicated that the reacted Fe/Ni 61.5 sample was composed of LP and/or GT and the Fe/Ni 14.9 sample contained GR (Fig. S8†). The presence of a GR-like phase was concluded from Raman spectra showing the typical Fe^{2+}–O and Fe^{3+}–O stretches at 400–500 cm^{-1} as well as a SO_4 band at 990 cm^{-1}.[35,52] The pH of formation for sulfated GR falls within our measured average pH range of 7.2–7.9. Its presence was unexpected as other works only report 6-line FH.[53]

3.3 Reactions at a target pH of 10 using 0.5 mM $Fe(II)_{(aq)}$

For the pure FH sample, the reaction pH range dropped to 7.5–8.1 and 99% of the total Fe (as $Fe(II)_{(aq)}$) was removed from solution by the end of the reaction period (Table 3). Phase analysis of the reacted FH solids *via* XRD showed no phase transformation, while micro-Raman spectroscopy detected the presence of LP (Fig. 3 and S9†).

For the As-FH cases, the decrease in pH from the target of 10 was significant for the Fe/As 4.47 sample (pH range 5.4–7.6) and moderate for Fe/As 32.9 (pH range 7.2–8.0). The Fe/As 32.9 sample showed no measurable As release to solution while the Fe/As 4.47 sample released an average of 10.1 ppm As. In both cases, 99% of the As remained in the solid phase (verified by the arsenate band at 853 cm^{-1}, Fig. 1) and an equal amount of the total Fe (as $Fe(II)_{(aq)}$) was removed from solution by the end of the 7-day reaction period. The measured concentration of As released into solution from the Fe/As 4.47 sample increased with time and did not readsorb onto the solid phase (Table 3). Similar As release behavior into solution was observed for the same $Fe(II)_{(aq)}$ concentration at a target pH of 8 (Table 2). Phase analysis of the reacted Fe/As 32.9 sample indicated only LP formed (Fig. 3 and S9†), and the Fe/As 4.47 sample again showed no phase transformation at the macro-scale (XRD, micro-Raman) or nano-scale (TEM) (Table S9, Fig. 3 and S10†).

The measured average pH range of the Fe/Mo 12.4 and Fe/Mo 31.5 samples over the reaction period was 8.6–8.7 and 7.7–8.8, respectively. For both samples, 99% of the Mo remained in the solid phase and an equal amount (99%) of total Fe (as $Fe(II)_{(aq)}$) was removed from solution by the end of the 7-day reaction period. An average of 491 and 46.1 ppm of Mo was released into solution by the end of day 7 from the Fe/Mo 12.4 and Fe/Mo 31.5 samples, respectively. The concentration of Mo released in both cases increased with time and was not readsorbed onto the solid phase (Table 3). No evident phase transformation for either the Fe/Mo 12.4 or Fe/Mo 31.5 samples was detected (from duplicate data) at the macro-scale (XRD, micro-Raman) or the nano-scale (TEM) (Tables 3 and S3, Fig. 3 and S10†). It has been reported that for FH reduction[14,15] at neutral pH values, the $Fe(II)_{(aq)}$ exists in solution as $FeOH^+$ ions, which accelerate the FH dissolution; however, at higher pH values (*e.g.*, pH 9) the amount of $FeOH^+$ ions decreases and as such may be why phase transformation is not observed at the set target pH of 10. Closer investigation of TEM images at higher resolution of the Fe/Mo 12.4 and Fe/Mo 31.5 samples revealed

Table 3 Leachability of Fe and elements of concern (X = As, Mo, and Ni) for tests conducted at pH 10 for 7 days with 0.5 mM $Fe(II)_{(aq)}$. Time 0 days represents conditions before Fe/X solids were added. Concentration units for (Fe) and (X) are in ppm. The values reported are the average of the two duplicate tests along with their standard deviations. Individual test data may be found in the ESI

Time	Ferrihydrite			Fe/As 4.47			Fe/As 32.9			Fe/Mo 12.4			Fe/Mo 31.2			Fe/Ni 14.9			Fe/Ni 61.5		
(days)	pH	(Fe)	(X)	pH	(Fe)	(X)	pH	(Fe)	(X)	pH	(Fe)	(X)	pH	(Fe)	(X)	pH	(Fe)	(X)	pH	(Fe)	(X)
0	5.5 ± 0.1	38 ± 0.07	0	5.5 ± 0	38 ± 0	0	5.5 ± 0	38 ± 0	0	5.5 ± 0	38 ± 0.1	0	5.5 ± 0.1	38 ± 0.1	0	5.5 ± 0	38 ± 0	0	5.5 ± 0	38 ± 0	0
1	7.9 ± 0.2	1.0 ± 1.0	0	5.6 ± 0.6	5.5 ± 0	1.5 ± 0.8	7.2 ± 2,0	5.2 ± 7.2	0	8.6 ± 0.1	0 ± 0.1	376 ± 0	8.7 ± 0.1	0 ± 0.1	8.2 ± 0.01	7.4 ± 0.2	43.1 ± 60.9	74.0 ± 17.2	7.8 ± 0.1	2.7 ± 0.7	5.3 ± 0.3
2	7.5 ± 0.4	0.2 ± 0.1	0	5.4 ± 0.6	2.0 ± 0	2.8 ± 1.2	7.6 ± 0.9	1.5 ± 2.0	0	8.6 ± 0.3	0 ± 0.1	375 ± 76.3	7.7 ± 0.1	0 ± 0.1	24.7 ± 0.01	8.0 ± 0.1	3.8 ± 5.4	10.7 ± 4.4	8.0 ± 0.1	1.2 ± 1.4	0.7 ± 0.4
4	8.1 ± 0.1	0 ± 0	0	7.3 ± 0.3	0.2 ± 0	6.8 ± 0	8.0 ± 0.9	0.2 ± 0.2	0	8.7 ± 0.3	0 ± 0.1	449 ± 28.9	8.7 ± 0.1	0 ± 0.1	35.4 ± 0.01	8.1 ± 0.1	2.4 ± 3.3	6.1 ± 2.0	8.0 ± 0.1	0.5 ± 0.1	0.8 ± 0.1
7	7.9 ± 0.1	0 ± 0	0	7.6 ± 0.1	0.1 ± 0	10.1 ± 0.49	7.9 ± 0.8	0.1 ± 0.1	0	8.7 ± 0.2	0 ± 0.1	437 ± 74.2	8.8 ± 0.1	0 ± 0.1	46.1 ± 0.1	8.2 ± 0.1	1.1 ± 1.5	1.7 ± 0.6	7.9 ± 0.1	0.4 ± 0.1	0 ± 0

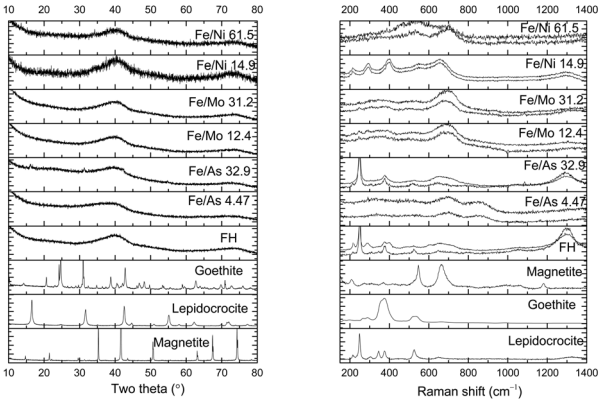

Fig. 3 Powder X-ray diffraction spectra (left) and micro-Raman spectra (right) of solid products reacted at a target pH of 10 for 7 days with 0.5 mM $Fe(II)_{(aq)}$. Spectra of relevant standard materials are shown for comparison. For each reacted sample, two Raman spectra are presented to show the mixtures of phases found in the reacted sample.

the starting formation of nanocrystalline elongated crystals typical of LP (Fig. S11†). This was surprising, especially for the Fe/Mo 31.5 sample, because phase transformation was observed for all other reaction conditions evaluated (Fig. 1, 2, S5, S7, and S10†). Such results indicate that, under the conditions evaluated, Mo (as MoO_4) adsorbed onto FH can significantly reduce the phase transformation at both high (Fe/Mo 12.4) and low (Fe/Mo 31.5) concentrations. This phenomenon is interesting because, to date, only covalently bonded molecules such as arsenates have been shown to impede/slow-down phase transformation of FH (adsorbed or co-precipitated).[12] However, we demonstrate here that non-covalently bonded molecules on FH (*e.g.*, Mo as MoO_4) may also demonstrate this effect under certain reaction conditions.

The measured average pH ranges for the Fe/Ni 14.9 and Fe/Ni 61.5 samples were 7.4–8.2 and 7.8–8.0, respectively. For both, 99% of the initial Ni remained in the solid while 97% and 99% of the total Fe (as $Fe(II)_{(aq)}$) was removed from solution for the Fe/Ni 14.9 and Fe/Ni 61.5 samples, respectively. The concentration of Ni released into solution was 74 ppm for the Fe/Ni 14.9 and 5.3 ppm for the Fe/Ni 61.5 sample. As observed for all other reaction conditions evaluated (Tables 1 and 2), Ni release into solution was greatest on the first day of reaction, after which it slowly decreased with time due to re-adsorption (Table 3) onto newly formed phases (*e.g.*, LP, GT, MG)[54] and/or unreacted FH (Fig. 3). Again no phase transformation was observed using XRD, while micro-Raman spectroscopic analysis indicated GT and MG for the Fe/Ni 14.9 sample but only MG for the Fe/Ni 61.5 sample (Table S9,† Fig. 3). This is notably different from the LP, GT, and GR-like phases observed at equimolar concentrations of 0.5 mM $Fe(II)_{(aq)}$ at a lower target pH of 8 (Fig. 2).[3]

4. Conclusions

For all X-FH (X = 0, As, Mo and Ni) cases studied here, the measured pH values were consistently lower than the target pH values of 8 and 10 despite daily re-adjustment; pH changes were

not buffered due to our use of saturated lime water as a base solution. Depending upon the X-FH composition, the decrease in pH from the target pH ranged from 1 to 5 pH units. The Fe/As 4.47 sample exhibited by far the highest pH decrease from the target pH (under all reaction conditions tested here), yet the Fe/Mo 12.4 and Fe/Ni 14.9 samples released larger amounts of adsorbed elements compared to the Fe/As samples. In all X-FH cases (X = As, Mo and Ni), an average of ≥98% of the X-element remained in the solid at the end of the 7-day reaction period.

Our control ferrihydrite behaved as expected and showed phase transformations to LP and GT under all reactions conditions tested. No magnetite was observed because the pH range for all the tests was ≤8. Furthermore, we were able to visually confirm that phase transformation to LP and/or GT does not occur homogenously on the surface of the reacted FH particles at the macro-scale.

With respect to As, inhibition of phase transformation was evident for the Fe/As 4.47 samples at the macro- and nano-scale under all reaction conditions tested, and As released into solution was not readsorbed onto the solid phase. The opposite was true for Fe/As 32.9, where no measurable As release into solution was detected and phase transformation to LP and/or GT phases was consistently observed.

With respect to Mo, phase transformation inhibition was observed for Fe/Mo 12.4 and Fe/Mo 31.5 samples at reaction concentrations of 0.5 mM $Fe(II)_{(aq)}$ and a target pH of 10. At a target pH of 8 and in the presence of low (0.5) or high (10 mM) $Fe(II)_{(aq)}$ concentrations, phase transformation to the expected LP and/or GT was observed. This is the first time that an outer-sphere bonding complex on FH (*e.g.*, Mo as MoO_4) has been demonstrated to inhibit/slow-down phase transformation of the FH to other crystalline Fe(II)–Fe(III)-hydroxide-oxide phases. Under all reaction conditions and for all Fe/Mo 12.4 and Fe/Mo 31.5 samples tested, Mo was released into solution regardless of whether phase transformation to LP and/or GT occurred or not. High Mo release into solution was observed for the Fe/Mo 12.4 samples reacted with concentrations of 0.5 mM $Fe(II)_{(aq)}$ at both target pHs (8 and 10). For both Fe/Mo samples reacted with 0.5 mM $Fe(II)_{(aq)}$, the Mo released from the solid into solution was not readsorbed even after 7 days of reaction and regardless of target pH. However, at concentrations of 10 mM $Fe(II)_{(aq)}$ and a target pH of 8, the Mo released into solution was readsorbed. Although the exact reason for the difference in Mo readsorption behavior observed here is not known, we postulate that there may be more Fe(III)–$Fe(II)_{(aq)}$ ions in solution at higher Fe(II) concentrations (10 mM) (from the reductive dissolution of FH) that can complex with some of the released Mo before its readsorption. In contrast, there may not be sufficient Fe(III)–$Fe(II)_{(aq)}$ ions in solution at lower $Fe(II)_{(aq)}$ concentrations to complex all of the Mo released into solution before it is readsorbed. Note that 99% of the Fe was removed by the end of the reaction period in both cases.

With respect to Ni, phase transformation to LP, GT, and/or MG was observed for Fe/Ni 14.9 and Fe/Ni 61.5 samples reacted under all conditions. At a target pH of 8 and concentrations of 0.5 mM $Fe(II)_{(aq)}$, the presence of a GR-like phase was observed for Fe/Ni 14.9. Under all reaction conditions and for both Fe/Ni 14.9 and Fe/Ni 61.5 samples, the largest amounts of Ni were released in solution on the first day of reaction and decreased thereafter. This readsorption behavior is attributed to the reattachment of the released aqueous Ni ions onto/into the newly formed solid phases (*e.g.*, LP, GT, MG, GR) and/or unreacted FH. This readsorption behavior is distinct from that of As and Mo, which are not readsorbed into new or unreacted solid phases after their release into solution except at high (10 mM) $Fe(II)_{(aq)}$ concentrations and a target pH of 8. The different readsorption behavior for Ni may arise from the fact that the complexation of Ni to FH can occur by three types of Ni–O–Fe covalent bonding. In contrast, only one type occurs for As-FH (covalent) and Mo-FH (non-covalent), giving Ni a better chance for readsorption by either unreacted FH or new Fe(III)(aq)-hydroxide-oxide solid phase(s). The pH of the solution can also affect the adsorption–desorption behavior of ions (*e.g.* As, Mo, Ni) with a substrate (*e.g.*, FH), but we believe this is not a significant factor here. This is because only the pH of the As-FH solution varied significantly compared to the Mo-FH and Ni-FH systems (the former of which was slightly higher).

The target pH of 8 was lower than the pH of the U mill and tailings operations of interest, which discharge tailings at a pH of 10. However, the lower target pH 8 conditions were of interest as they are more applicable to conditions that may be encountered in natural systems as well as also other U-mill and tailings operations that employ near neutral pH conditions. While the systems with a target pH of 10 often had pH values that were not considerably different than those with a target pH of 8, the reacting conditions (and therefore their behavior in terms of phase transformation and X element release) were distinct as a result of the daily readjustment of the pH to 10 (daily shock to the system); with the exception of the As system, the experiments at a target pH of 8 tended to stay around their set pH target value.

Lastly, the results presented in this study enabled us to evaluate the stability of such X-FH (X = 0, As, Mo and Ni) varieties in terms of phase stability-transformation and TCLP-like leachability under abiotic anoxic conditions over a range of set pH target values typically found in natural and man-made (mining) systems. The data on the synthetic X-FH systems (especially for Mo and Ni where no data exists) allow us to begin to understand how more complex systems (*e.g.*, mine tailings) composed of multiple phases (*e.g.*, As-FH, Ni-FH, Mo-FH, and other metal hydroxides-oxides) will behave if they are subjected to anoxic conditions, release $Fe(II)_{(aq)}$ ions, and undergo phase transformation. Indeed, future work using the same conditions as this study will be conducted on more complex U-tailings to compare with the behaviors reported here.

Acknowledgements

Financial support for the study was provided by Cameco Corporation and the Natural Sciences and Engineering Research Council of Canada (NSERC) through a Senior Industrial Research Chair to MJH. Assistance received from F. Nelson, J. Fan and Tom B (Geological Sciences), J. Maley and P. Wennek (Chemistry), and the Saskatchewan Structural Sciences Centre (SSSC) located at the University of Saskatchewan is

acknowledged. We also thank Dr M. Celikin (Mining and Materials Engineering, McGill University) for conducting the TEM analyses.

Notes and references

1 R. M. Cornell and U. Schwertmann, Cation substitution, in *The iron oxides: structure, properties, reactions, occurrence and uses*, VCH, Weinheim, Germany, 1996, pp. 35–52.
2 J. R. Lloyd, *FEMS Microbiol. Rev.*, 2003, **27**(2–3), 411.
3 C. M. Hansel, S. G. Benner and S. Fendorf, *Environ. Sci. Technol.*, 2005, **39**, 7147.
4 R. Schaetzl and S. Anderson, *Soils: Genesis and Geomorphology*, Cambridge University Press, Cambridge, UK, 2005, p. 817.
5 G. C. Murray and D. Hesterberg, *Soil Sci. Soc. Am. J.*, 2006, **70**(4), 1318.
6 N. R. Posth, F. Hegler, K. O. Konhauser and A. Kappler, *Nat. Geosci.*, 2008, **1**(10), 703.
7 R. M. Handler, B. L. Beard, C. M. Johnson and M. M. Scherer, *Environ. Sci. Technol.*, 2009, **43**, 1102.
8 D. A. Lipson, M. Jha, T. K. Raab and W. C. Oechel, *J. Geophys. Res.*, 2010, **115**, 2156.
9 L. Yang, C. I. Steefel, M. A. Marcus and J. R. Bargar, *Environ. Sci. Technol.*, 2010, **44**, 5469.
10 C. A. Gorski and M. M. Scherer, Fe^{2+} sorption at the Fe oxide–water interface: A revised conceptual framework, in *Aquatic Redox Chemistry*, American Chemical Society, 2011, vol. 1071, pp. 315–343.
11 H. D. Pedersen, D. Postma and R. Jakobsen, *Geochim. Cosmochim. Acta*, 2006, **70**, 4116.
12 J. J. Erbs, T. S. Berquó, B. C. Reinsch, G. V. Lowry, S. K. Banerjee and R. L. Penn, *Geochim. Cosmochim. Acta*, 2010, **74**, 3382.
13 Y. Masue-Slowey, R. H. Loeppert and S. Fendorf, *Geochim. Cosmochim. Acta*, 2011, **75**, 870.
14 H. Liu, P. Li, M. Zhu, Y. Wei and Y. Sun, *J. Solid State Chem.*, 2007, **180**, 2121.
15 H. Liu, P. Li, B. Lu, Y. Wei and Y. Sun, *J. Solid State Chem.*, 2009, **182**, 1767.
16 J. Jang, B. A. Dempsey, G. L. Catchen and W. D. Burgos, *Colloids Surf., A*, 2003, **221**, 55.
17 D. E. Latta, J. E. Bachman and M. M. Scherer, *Environ. Sci. Technol.*, 2012, **46**, 10614.
18 J. A. Frierdich and J. G. Catalano, *Environ. Sci. Technol.*, 2012a, **46**, 11070.
19 J. A. Frierdich and J. G. Catalano, *Environ. Sci. Technol.*, 2012b, **46**, 1519.
20 K. Amstaetter, T. Borch, P. Larese-Casanova and A. Kappler, *Environ. Sci. Technol.*, 2010, **44**, 102.
21 C. M. Hansel, C. R. Learman, C. J. Lentini and E. B. Ekstrom, *Geochim. Cosmochim. Acta*, 2011, **75**, 4653.
22 P. Landine, Cameco Rabbit Lake in-pit tailings management facility-tailings injection trail program, in *The Long Term Stabilization of Uranium Mill Tailings* (Final report of a coordinated research project), IAEA-TECDOC-1403, IAEA, Vienna, 2004, pp. 121–144.
23 S. A. Shaw, M. J. Hendry, J. Essilfie-Dughan, T. Kotzer and D. Wallschläger, *Appl. Geochem.*, 2011, **12**, 2044.
24 B. J. Moldovan, M. J. Hendry and G. A. Harrington, *Appl. Geochem.*, 2008, **23**, 1437.
25 T. Pichler, M. J. Hendry and G. E. M. Hall, *Environ. Geol.*, 2001, **40**, 495.
26 B. J. Moldovan and M. J. Hendry, *Environ. Sci. Technol.*, 2005, **39**, 4913.
27 B. J. Moldovan, D. T. Jiang and M. J. Hendry, *Environ. Sci. Technol.*, 2003, **37**, 873.
28 J. Mahoney, M. Slaughter, D. Langmuir and J. Rowson, *Appl. Geochem.*, 2007, **22**, 2758.
29 J. Essilfie-Dughan, I. J. Pickering, M. J. Hendry, G. N. George and T. Kotzer, *Environ. Sci. Technol.*, 2011, **45**, 455.
30 J. Essilfie-Dughan, J. Hendry, J. Warner and T. Kotzer, *Geochim. Cosmochim. Acta*, 2012, **96**, 336.
31 G. Heinrich, K. Kyser, D. Chipley and E. Lam, The determination of selenium and molybdenum distribution in uranium ore and mill solids, in *Proceedings of the 3rd International Conference on Uranium (Uranium 2010)*, ed. E. K. Lam, J. W. Rowson and E. Özberk, Saskatoon, SK, Canada, August 15–18, 2010, vol. 1, p. 609.
32 Atomic Energy Control Board, *Regulatory Objectives, Requirements and Guidelines for the Disposal of Radioactive Wastes – Long-term Aspects*, Ottawa, Canada, 1987.
33 D. Langmuir, J. Mahoney, A. MacDonald and J. Rowson, *Geochim. Cosmochim. Acta*, 1999, **63**, 3379.
34 D. Langmuir, J. Mahoney and J. Rowson, *Geochim. Cosmochim. Acta*, 2006, **70**, 2942.
35 I. A. M. Ahmed, L. G. Benning, G. Kakonyi, A. D. Sumoondur, N. J. Terrill and S. Shaw, *Langmuir*, 2010, **26**, 6593.
36 US-EPA, *Developments for In Situ Treatment of Metal Contaminated Soils*, http://www.clu-in.org/download/remed/metals2.pdf, 1997.
37 D. L. Bish and S. J. Chipera, Accuracy in quantitative X-ray powder diffraction analyses, *Advances in X-ray Analysis*, ed. P. Predecki *et al.*, Plenum Pub. Co., 1995, vol. 38, pp. 47–57.
38 L. Mazzetti and P. J. Thistlethwaite, *J. Raman Spectrosc.*, 2002, **33**, 104.
39 M. L. Franquelo, A. Duran, L. K. Herrera, M. C. Jimenez de Haro and J. L. Perez-Rodriguez, *J. Mol. Struct.*, 2009, **924–926**, 404.
40 G. A. Jenner, H. P. Longerich, S. E. Jackson and B. J. Fryer, *Chem. Geol.*, 1990, **83**, 133.
41 H. P. Longerich, G. Jenner, B. Fryer and S. Jackson, *Chem. Geol.*, 1990, **83**, 105.
42 N. Yee, S. Shaw, L. G. Benning and T. H. Nguyen, *Am. Mineral.*, 2006, **91**, 92.
43 E. Krause and V. A. Ettel, *Am. Mineral.*, 1988, **73**, 850.
44 J. E. Katz, X. Zhang, K. Attenkofer, K. W. Chapman, C. Frandsen, P. Zarzycki, K. M. Rosso, R. W. Falcone, G. A. Waychunas and B. Gilbert, *Science*, 2012, **337**(6099), 1200.
45 G. A. Waychunas, B. A. Rea, C. C. Fuller and J. A. Davis, *Geochim. Cosmochim. Acta*, 1993, **57**, 225.

46 L. Brinza, L. G. Benning and P. J. Statham, *Mineral. Mag.*, 2008, **72**, 107.
47 L. Brinza, Interactions of molybdenum and vanadium with iron nanoparticles, PhD thesis, University of Leeds, West Yorkshire, UK, June 2010.
48 Y. Arai, *Environ. Sci. Technol.*, 2008, **42**, 1151.
49 K. B. Burgess and D. J. Lowe, *Chem. Rev.*, 1996, **96**(7), 2983.
50 L. H. G. Chaves, J. E. Curry, D. A. Stone and J. Chorover, *Rev. Bras. Cienc. Solo*, 2007, **31**, 813.
51 P. Refait and J. M. R. Genin, *Clays Clay Miner.*, 1997, **32**, 597.
52 L. Legrand, G. Sagon, S. Lecomte, A. Chausse and R. Messina, *Corros. Sci.*, 2001, **43**, 1739.
53 R. K. Kukkadapu, J. M. Zachara, J. K. Fredreickson, S. C. Smith, A. C. Dohnalkova and C. K. Russell, *Am. Mineral.*, 2003, **88**, 1903.
54 N. Gokon, N. Hasegawa, H. Kaneko, T. Ohara and Y. Tamaura, *J. Magn. Magn. Mater.*, 2003, **256**, 293.